3D handheld scanning to quantify head shape changes in spring assisted surgery for sagittal craniosynostosis

Maik Tenhagen[1,2], Jan L Bruse[1,3], Naiara Rodriguez-Florez[1,2], Freida Angullia[1,2], Alessandro Borghi[1,2], Maarten J Koudstaal[1,4], Silvia Schievano[1,2,3], NU Owase Jeelani[1,2], David Dunaway[1,2]

[1] *Great Ormond Street Hospital for Children, London, United Kingdom*

[2] *University College London Institute of Child Health, London, United Kingdom*

[3] *University College London Institute of Cardiovascular Science, London, United Kingdom*

[4] *Erasmus Medical Centre, Maxillofacial Surgery, Rotterdam, The Netherlands*

Corresponding author:

David Dunaway,

Craniofacial Unit

Great Ormond Street Hospital for Children,

Great Ormond Street,

London WC1N 3JH,

United Kingdom

Tel.: +44 (0) 20 7405 9200

Fax: +44 (0) 20 7813 8446

Keywords: 3D handheld scanning, statistical shape modelling, scaphocephaly, spring-assisted surgery.

Abstract (max 250 words)

Three-dimensional (3D) imaging is an important tool for diagnostics, surgical planning and evaluation of surgical outcomes in craniofacial procedures. Gold standard for acquiring 3D imaging is computed tomography (CT) which entails ionizing radiations and, in young children, a general anaesthesia. 3D photographic imaging is an alternative method to assess patients who have undergone calvarial reconstructive surgery. The aim of this study was to assess the utility of 3D handheld scanning photography in a cohort of patients that underwent spring-assisted correction surgery for scaphocephaly. Pre- and post-operative 3D scans acquired in theatre and at the 3-week follow-up in clinic were post-processed for 9 patients. Cephalic index (CI), head circumference, volume, sagittal length and coronal width over the head at pre-op, post-op and follow-up were measured from the 3D scans. CI from 3D scans were compared with measurements from planar x-rays. Statistical shape modelling (SSM) was used to calculate the 3D mean anatomical head shape of the 9 patients at the pre-op, post-op and follow-up. No significant differences were observed in the CI between 3D and x-ray. CI, volume and coronal width increased significantly over time. Mean shapes from SSM visualized the overall and regional 3D changes due to the expansion of the springs in situ. 3D handheld scanning followed by SSM proved to be an efficacious and practical method to evaluate 3D shape outcomes after spring assisted cranioplasty in individual patients and in the population.

1. Introduction

Three-dimensional (3D) imaging is an important tool for diagnosis of craniofacial disorders, planning of surgical treatments and evaluation of surgical outcomes. Computed tomography (CT) is the imaging gold standard, due to its ability of displaying hard tissue with high spatial resolution. Multiple CT scans to monitor surgical progress are undesirable due to the cumulative x-ray exposure[1] and the need for general anaesthesia in young children. CT examinations are therefore confined to selected situations in which CT associated risks are counterbalanced by the clinical needs to study the complex problem [2].

3D photography is an alternative, non-invasive method to acquire surface information of the human body. The methodology has been successfully applied in cranio-maxillofacial studies to assess soft tissue changes following treatments such as helmet therapy [3] or surgeries [4, 5], to identify facial phenotypes in patient populations [6] and quantify cranial facial proportions [7]. However, most current systems require highly specialised equipment, placed in a dedicated room in a fixed position, and trained staff to acquire and process the images. Portable 3D handheld scanners are now available that allow capturing 3D models of the human body by moving the scanner around the region of interest to acquire its entire surface. These compact, non-invasive systems have the potential to acquire the patient specific 3D head shape to quantify surgical outcomes in the operating theatre and monitor follow-up results [8-11] during clinics in craniofacial applications.

Spring-assisted cranioplasty was introduced by Lauritzen in 1998 [12] as a minimally invasive technique to treat sagittal craniosynostosis. The technique has been developed by several institutions including Great Ormond Street Hospital for Children (GOSH, London, UK) where standardised springs are placed in predefined positions. The corrective effects of spring assisted cranioplasty occur both at the time of surgery and for a variable period of time after surgery, as the skull gradually deforms due the latent force stored within the springs. 3D CT imaging is not routinely used at GOSH for children undergoing this intervention, and traditionally, analysis of the head shape change is based on clinical evaluation and

planar x-rays, with 2D measurement of head shape change via cephalic index (CI) [13-16]. 3D photography using handheld devices could enhance our understanding of the head shape changes induced by springs over time.

We present a non-invasive, radiation-free and portable tool to quantify the 3D head shape changes induced by spring-assisted cranioplasty in children with sagittal synostosis. 3D based cephalometric measurements were first compared with those retrieved from conventional planar imaging. The analysis was extended to investigate the potential of 3D imaging using non-landmark based shape analysis to assess the overall outcome of the procedure and regional shape changes over time on a population-averaged model [17].

2. Materials and Methods

Patient population and procedure

Between May and October 2015, 12 patients undergoing spring-assisted cranioplasty for sagittal craniosynostosis at GOSH were prospectively enrolled in the study. Patients presented with isolated sagittal craniosynostosis and scaphocephaly, confirmed by clinical examination and pre-procedural x-rays. Images of the calvarium shape were acquired pre- and post-operatively in theatre, and at follow-up in clinic using a 3D handheld scanner. During image post-processing analysis, three patients were excluded from the overall study due to poor image quality at one of the three time points. The mean age at surgery of the remaining 9 patients – 1 female – was 5.2±1 months (Table 1). Parents/guardians gave informed consent for the use of the data for research purposes.

Spring assisted surgery was undertaken with the patient in the prone position through a transverse scalp incision midway between the anterior and posterior fontanel. After a 1.5 cm square craniectomy, performed halfway along the sagittal suture, two parasagittal osteotomies were made approximately 7 mm from the midline, extending from the coronal to the lambdoid sutures. Two standardised metal springs (Active Spring Company, Thaxted, UK) were inserted into small notches made in the parietal bone on each side of the osteotomy (Figure 1). Three spring wire diameters are available (S10, S12 and S14) with increasing stiffness: 5 patients received S12 in both the anterior and posterior position, 3 patients S14 in both positions, and one patient had S12 anteriorly and S14 posteriorly (Table 1). Patients were followed up with x-rays after surgery and at the first outpatient clinic appointment, approximately 3 weeks (22±5 days) later in order to monitor the opening and position of the springs, and the changes in CI. Spring opening was measured for each patient at the time of insertion on the table and from the 3-week follow-up x-rays (Table 1).

3D scanning and image post-processing

A structured light handheld scanner, the M4D Scan 3D scanner provided by Rodin4D (Pessac, Acuitaine, France), was used for the acquisition of the 3D calvarium shape. Structured light scanners reflect a pattern of light on the target surface and use the difference detected by two cameras in the scanner to compose the 3D model. A white nylon stocking (Beagle Orthopaedic, UK) was placed on the head of the patients to overcome the difficulties of the scanner in capturing hair. VXelements (Creaform, Levis, Quebec, Canada) software was used in conjunction with the 3D camera during the acquisition to assess the result in real time. Files were exported from the software as 3D computational surface meshes in STL format. These STL files contained information about point coordinates and connections between points that form the shape of the head.

3D scans were acquired by the same operator at three time points:

- pre-operatively: immediately before the start of surgery, with the patient under general anaesthesia and located on the operating table in sphinx position;
- post-operatively: immediately after surgery and cleaning of the patient, with the child still located in sphinx position on the operating table; and
- follow-up: three weeks after surgery, during the first outpatient follow-up appointment in clinic.

After acquisition, the raw output mesh files from VXelements were processed offline to clean, merge and register the 3D surfaces before further analysis (Figure 2a-b). First, MeshMixer (Autodesk Research, Toronto, Canada) was used to clean up noise due to surrounding structures. If multiple scans were taken of the same patient at the same time point, the incomplete scans were loaded into 3-matic® (Materialise, Leuven, Belgium) where they were registered with each other using a combination of N-point (5-6 manually selected reference anatomical landmarks) and global registration algorithms, before merging them into one complete 3D scan.

Second, the seams of the stocking were smoothed out and the holes around the ears were filled to ensure that the volume of the 3D mesh could be calculated properly.

Third, the lower border of the patient head model was defined to ensure an easily and consistently identifiable cutting plane. Despite the Frankfort horizontal plane being the most widely used plane for anatomical positioning of the human skull [18], a cutting plane through the nasion and both tragion points was chosen to include the whole occiput in this study (Figure 2c). This allowed the analysis of occipital bossing in patients with scaphocephaly (Figure 3).

Accurate registration of the different patient and different time point scans, essential for meaningful 3D morphometric analysis, was achieved using the 3 same landmark points used for the cutting planes (nasion and both tragion points) and an additional landmark on the most posterior and medial point of the cutting plane. All pre-operative scans from the nine patients were registered using an N-point registration algorithm in 3-matic®, and for each patient, the post-operative and follow-up scans were registered to the corresponding pre-operative scan.

To compare the use of the 3D handheld scanner for cephalometric measurements to currently used techniques, CI was measured on both the 3D scans and the x-rays.

The following additional conventional measurements were performed from the 3D scans (Figure 2d) [19, 20] to assess the results of the procedure:

- head circumference, measured using the glabella and occipital prominence as identifiers;
- sagittal length from the nasion, in the sagittal plane, all the way over the head;
- coronal width over the head from the left to the right tragion in the coronal plane; and
- volume under the mesh surface capped by the cutting plane.

Statistical Shape Analysis

Statistical shape modelling (SSM) was carried out using the registered 3D surface meshes to compute 3D anatomical mean shapes for the population [21]. Due to the absence of distinct anatomical landmarks on the scalp, a *non-parametric* SSM approach was used, which enables the analysis of smooth continuous shapes without the need for landmarking or point-to-point correspondence between them – a technique previously applied in studies of endocranial shapes of bonobos and chimpanzees [17]. All shape analysis was carried out within the Deformetrica shape modelling framework [22] (www.deformetrica.org). The software computes the 3D mean anatomical shape of a population (template shape). The deformation vectors required to recreate the shape of each individual head in the population from the template shape are then calculated. Each individual head shape is thus defined by the mean shape and a unique deformation vector. The great advantage of this technique is that head shape can be described without the need for homologous landmarks, which are impossible to find accurately on the posterior skull.

Using the 3D scans of the 9 patients at the three time points as input shapes, the 3D anatomical mean shape for each of the three stages was computed [23]. The computed mean shapes were validated against population averages of CI, head circumference, sagittal length, coronal width and head volume.

For the computed mean shapes from the SSM and for each patient, surface distances between the post-operative and the pre-operative models, as well as between the follow-up and the pre-operative models were calculated using VMTK [24] (*www.vmtk.org*). Respective distance colour maps were generated in ParaView [25] to visualize and analyse postsurgical local shape changes.

Statistical analysis

Statistical tests were performed using IBM® SPSS® Statistics version 22.0 (SPSS Inc., Chicago, IL). A Bland-Altman plot was used to analyse agreement between x-ray and 3D scan for assessment of CI. The Wilcoxon signed-rank test with a significance level of $p=0.05$ was used for the comparison between the 3D anatomical template and the average of the population for all cephalometric measurements, and for the

cephalometric measurement and spring opening changes at the different time points. The independent sample Mann -Whitney *U* test was used for comparison of S12 vs S14 opening.

3. Results

Confident use of the handheld scanner in acquiring adult volunteer head shapes required a short amount of training. However, a few challenges presented when scanning the infants, both under general anaesthesia on the operating table and while awake in clinic. Time pressure in the operating theatre resulted in an acquisition time of less than 5 minutes for a complete 3D scan, including setting up the system, applying the nylon cap and the scanning process itself, at the expense of image quality which in some cases turned to be quite low. When exported and analysed at the computer, three patients were indeed discarded from the study as the quality of their post-operative scans was considered not suitable for further processing, i.e. landmarking point for definition of cutting plane was missing, large holes were present in the surface or artefacts such as double surfaces were identified (Figure 3).

The scanning process at the 3-week follow-up appointment in clinic proved more challenging compared to the same procedure in the operating room, mainly due to movements of the patients who were attracted by the scanner projecting light. This resulted in the scanner losing signals for short periods of time. However, the lack of time constraints in the waiting room for the follow-up appointments allowed for multiple acquisitions of each child head and in turns better image quality. A light toy proved helpful in focusing the infants' attention during acquisition, thus reducing their head movements and, therefore, scanning time, which remained always within 10 minutes.

After acquisition, the preparation of the surface scans into final volumes for measurement and morphometric analysis relied on a manual process requiring between 45 and 60 operator minutes per 3D scan, according to the initial quality of the acquired images.

Spring measurements at insertion on table and from follow-up x-ray showed the expected behaviour of the devices with opening increasing over time (37 ± 4 mm immediate post-op to 54 ± 3 mm at follow-up, $p < 0.001$). The posterior springs widened more than their anterior counterparts at insertion (39 ± 5 vs 36 ± 4 mm, $p = 0.016$), but there were no significant differences at follow-up (54 ± 4 vs 55 ± 3 mm, p =

0.796) meaning that both anterior and posterior springs open widely with time. In this small cohort of cases, S12 springs were implanted in younger patients, while S14 were reserved for older patients. In those cases where S14 were used, the trends showed that despite the stiffer spring, there was slightly less opening at follow-up compared to the S12 cases (52 ± 4 vs 56 ± 2 mm, p = 0.035) but no important difference on table (35 ± 4 vs 39 ± 4 mm, p = 0.056).

The Bland-Altman plot for CI agreement between x-ray and 3D scans showed a mean difference of -1.17% and no visible trends (Figure 4). CI increased from 70 ± 2.9% to 71.5 ± 3.3% between pre-op and immediate post-op measurements, and to 74 ± 4.3% at follow-up (Figure 5). The increase in CI was significant for pre-op to post-op, pre-op to follow-up and post-op to follow-up (Table 2).

Average volume, sagittal length, coronal width and circumference in the population at the three time points (pre, post and follow-up) are plotted in Figure 6. The results of the statistical analysis are shown in Table 2. Significant increases were found for both coronal width and volume pre-op to post-op, pre-op to follow-up and post-op to follow-up. No significant differences were found for sagittal length, and the head circumference only increased significantly for post-op to follow-up.

3D scans at pre, post and follow-up of 9 sagittal craniosynostosis patients allowed for both a patient specific and a population based analysis. Colour maps of each patient showed the individual shape change after spring-assisted cranioplasty. Immediately after insertion, patient 5 had the smallest measured anterior and posterior spring openings and indeed on the 3D scan colour maps the changes were small, whilst patient 9 had one of the largest expansions as highlighted also by the red areas in the 3D scan. At 3-week follow-up, patient 8 had the smallest overall spring opening and one of the lowest 3D shape changes, whilst patient 2 had the largest spring opening, in particular for the posterior spring, shown by the red areas located mainly in the posterior portion of the calvarium. Apart from demonstrating the expected effect of spring assisted cranioplasty in widening the head, the individual colour maps also

highlighted common trends in the development of bi-parietal prominences and the small negative change around the frontal region.

The computed mean head shapes for each time-point showed overall features similar to the individual scans (Figure 8). Positive differences were found bilaterally around the vertex and were in the range of 5 mm at post-op and 7 mm at follow-up scans. Negative differences were found in the frontal region to a maximum of approximately 2 mm at follow-up.

Differences between the population averaged cephalometric measurements and those from the 3D template model representing the 3D mean shape of the population were all < 1.5%, demonstrating that the mean head template was a good representation of the 3D shape average of the population.

4. Discussion

Rodin4D optical structured light 3D scanner proved to be an effective method of capturing head shape. The high portability of the handheld scanner allowed acquisition of 3D images in theatre and during patient appointments, in fairly short times. A few training test cases were enough to confidently acquire good quality images of head shapes from cooperating adults, and albeit head movements when scanning awake infants required longer acquisition times, the full process from setting up the camera to acquiring the full head shape remained below 10 minutes.

The 3D scanning techniques based on the use of structured light have been tested on accuracy and precision before [26]. One study has compared CI from optical 3D scans with CT and manual measurements [27]. Van Lindert et al. [27] compared CI measured through several techniques and concluded that measurement on optical 3D scans possibly becomes the method of first choice as they are non-irradiating, reliable and reproducible. Our study found a high degree of agreement between CI calculated from optical scans and conventional methods and support their conclusion.

One disadvantage of the technique was the considerable amount of post-acquisition image processing that was required to produce useable images. 3D data unintentionally sampled from the surrounding environment needed to be removed and where the entire volume was not captured in one scan, a further processing step was required to "stitch" together two sequentially captured scans. Lastly, small voids in the scan surface had to be filled in to allow an analysis of overall surface leading to possible inaccuracies in the data.

A novel aspect of this study was the use of a non-parametric, no point-to-point based analysis of the 3D surfaces. Many techniques have been described to assess head and skull shape, and almost all of them depend to some degree on a point-based analysis. In order for this to be meaningful, reproducible identifiable homologous points must be recognised. Identifying numerous homologous points in complex shapes such as the face or facial skeleton is straightforward, but is almost impossible in smooth, feature

poor objects such as the calvarium. Historically, this problem has been addressed by creating secondary points (e.g. the midpoint between two homologous points)[28]; however, derived points such these compound inaccuracies in the analysis. The technique employed in this study set a cutting reference plane between three points (nasion and tragions), used to define the limits of the surface of interest in the same manner for all subjects and to register the scans. After that, shape analysis was entirely non-point based, and looked at the variation of shape for each patient over time and at the construction of mean population models.

Changes in cephalic index have been widely reported as outcome after spring-assisted correction of sagittal craniosynostosis [13, 16, 19, 29, 30]. In this study, mean CI increased from 70 preoperative to 74 at the 3-week follow-up. These values are similar to previous studies, reporting increases in CI from 66-67 preoperatively to 75-76 at long term follow-up [13, 16, 19]. David *et al* (2010) [19] concluded that CI, although the most commonly quoted outcome measure, provides limited information about global change in head shape. An improvement in CI infers an improvement in the degree of scaphocephaly, but ignores many of the other stigmatising features of scaphocephaly such as frontal bossing, occipital prominence and adverse cranial height [31].

Although this was a small cohort study, the developed methodology allowed understanding of some trends in spring assisted cranioplasty. The procedure produced a small increase in cranial volume (6.7% after 3 weeks) which is of great importance in a condition that can lead to raised intracranial pressure due to cranio-cerebral disproportion. A small increase in head circumference was found, which was seen immediately post operatively in the operating room and became more marked 3 weeks postoperatively. Because of the short follow-up time span, these effects were likely to be almost entirely due to the procedure with a negligible contribution from natural head growth.

The colour maps showing shape change for each individual head from pre-op to immediate post-op and from pre-op to follow-up are particularly informative. They demonstrated that insertion of springs

produced an immediate postoperative change in head shape consisting of a bi-parietal expansion, and thus an increased coronal width, accompanied by a small decrease in cephalic length caused principally by a recession of the forehead. Three weeks postoperatively, there was further change, more distributed along the head. Whether this represents further viscoelastic change or early biological remodelling of the skull could not be ascertained by this study. The colour maps also revealed that the change in cephalic index was principally a result of the increase in the bi-parietal width rather than the reduction of the antero – posterior distance. In order to effectively treat scaphocephaly both length and width of the skull must be addressed and spring assisted cranioplasty appears to be only partially effective in this respect. Interestingly, the colour maps showed a tendency for shape change to occur asymmetrically which reflected the slight unpredictability of the surgical technique.

The greatest shape change had occurred in the superior parietal region, as demonstrated in the colour maps. The analysis presented in this paper measures distance between the closest points on the two surfaces being compared. Examination of the axial and lateral shape models demonstrated that the change in this area was due both to a widening of the head and an increase in calvarial height, both of which are desirable characteristics.

Construction of a statistical shape model and calculation of the population mean shapes revealed further quantitative and localised descriptive information on the effects of spring cranioplasty. Bi-parietal expansion immediately after insertion was localised more towards the back of the head in correspondence to the posterior spring, which on table opened more compared to the anterior spring. At follow-up the mean model showed further changes, more distributed on the entire head, with further bilateral expansion more towards the central portion of the calvarium.

Structured light handheld 3D scanners provide a convenient and effective way of capturing head shape. Non-parametric statistical shape modelling facilitates accurate analysis of the head shape and the changes that occur with surgery. In this study, these techniques have been used to investigate the effects of spring

assisted cranioplasty for the treatment of sagittal craniosynostosis. The detailed shape analysis has the potential to highlight systematic overall problems with spring-assisted cranioplasty and patient specific local regional shape changes that could help drive modifications of the surgical technique and improvement of the spring device in the future.

5. Conflicts of Interest

None.

6. Acknowledgements

This research was supported by GOSH charity through the FaceValue programme grant, Fondation Leducq and the grants from the Erasmus University and A.A. van Beek-fund.

This report incorporates independent research from the National Institute for Health Research Biomedical Research Centre Funding Scheme. The views expressed in this publication are those of the author(s) and not necessarily those of the NHS, the National Institute for Health Research or the Department of Health.

7. References

1. Almohiy, H., *Paediatric computed tomography radiation dose: A review of the global dilemma.* World J Radiol, 2014. 6(1): p. 1-6.
2. Fearon, J.A., et al., *The diagnosis and treatment of single-sutural synostoses: are computed tomographic scans necessary?* Plast Reconstr Surg, 2007. 120(5): p. 1327-31.
3. Schaaf, H., et al., *Three-dimensional photographic analysis of outcome after helmet treatment of a nonsynostotic cranial deformity.* J Craniofac Surg, 2010. 21(6): p. 1677-82.
4. Chan, F.C., et al., *Soft-tissue volumetric changes following monobloc distraction procedure: analysis using digital three-dimensional photogrammetry system (3dMD).* J Craniofac Surg, 2013. 24(2): p. 416-20.
5. Chen, Z.C., et al., *Precision of three-dimensional stereo-photogrammetry (3dMD) in anthropometry of the auricle and its application in microtia reconstruction.* J Plast Reconstr Aesthet Surg, 2015. 68(5): p. 622-31.
6. Aldridge, K., et al., *Facial phenotypes in subgroups of prepubertal boys with autism spectrum disorders are correlated with clinical phenotypes.* Mol Autism, 2011. 2(1): p. 15.
7. Skolnick, G.B., et al., *Comparison of Direct and Digital Measures of Cranial Vault Asymmetry for Assessment of Plagiocephaly.* J Craniofac Surg, 2015. 26(6): p. 1900-3.
8. Dixon, T.K., et al., *Three-dimensional evaluation of unilateral cleft rhinoplasty results.* Facial Plast Surg, 2013. 29(2): p. 106-15.
9. Largo, R.D., et al., *Three-dimensional laser surface scanning in rhinosurgery.* Facial Plast Surg, 2013. 29(2): p. 116-20.
10. Freudlsperger, C., et al., *Metopic synostosis: Measuring intracranial volume change following fronto-orbital advancement using three-dimensional photogrammetry.* J Craniomaxillofac Surg, 2015. 43(5): p. 593-8.

11. Weathers, W.M., et al., *A novel quantitative method for evaluating surgical outcomes in craniosynostosis: pilot analysis for metopic synostosis.* Craniomaxillofac Trauma Reconstr, 2014. 7(1): p. 1-8.

12. Lauritzen, C., et al., *Spring mediated dynamic craniofacial reshaping. Case report.* Scand J Plast Reconstr Surg Hand Surg, 1998. 32(3): p. 331-8.

13. Davis, C., A. Wickremesekera, and M.R. MacFarlane, *Correction of nonsynostotic scaphocephaly without cranial osteotomy: spring expansion of the sagittal suture.* Childs Nerv Syst, 2009. 25(2): p. 225-30.

14. Mackenzie, K.A., et al., *Evolution of surgery for sagittal synostosis: the role of new technologies.* J Craniofac Surg, 2009. 20(1): p. 129-33.

15. Shen, W., et al., *Correction of craniosynostosis using modified spring-assisted surgery.* J Craniofac Surg, 2015. 26(2): p. 522-5.

16. van Veelen, M.L. and I.M. Mathijssen, *Spring-assisted correction of sagittal suture synostosis.* Childs Nerv Syst, 2012. 28(9): p. 1347-51.

17. Durrleman, S., et al., *Comparison of the endocranial ontogenies between chimpanzees and bonobos via temporal regression and spatiotemporal registration.* J Hum Evol, 2012. 62(1): p. 74-88.

18. Lundström, A., Lundström, F., *The Frankfort horizontal as a basis for cephalometric analysis.* Am J Orthod Dentofacial Orthop, 1995 107(5): p. 4.

19. David, L.R., et al., *Outcome analysis of our first 75 spring-assisted surgeries for scaphocephaly.* J Craniofac Surg, 2010. 21(1): p. 3-9.

20. Linz, C., et al., *3D stereophotogrammetric analysis of operative effects after broad median craniectomy in premature sagittal craniosynostosis.* Childs Nerv Syst, 2014. 30(2): p. 313-8.

21. Pennec, X., *Statistical Computing on Manifolds: From Riemannian Geometry to Computational Anatomy.* Emerging Trends in Visual Computing, 2009(2009): p. 40.

22. Durrleman, S., et al., *Morphometry of anatomical shape complexes with dense deformations and sparse parameters.* Neuroimage, 2014. 101: p. 35-49.

23. Bruse, J., et al., *A statistical shape modelling framework to extract 3D shape boiomarkers from medical imaging data: assessing arch morphology of repaired coarctation of the aorta*, BMC Med Imaging, 2016. 16:40

24. Antiga, L., et al., *An image-based modeling framework for patient-specific computational hemodynamics.* Med Biol Eng Comput, 2008. 46(11): p. 1097-112.

25. Ahrens, J., Geveci, B., Law, C., *ParaView: An End-User Tool for Large-Data Visualization.* The Visualization Handbook, 2005(2005).

26. Ma, L., T. Xu, and J. Lin, *Validation of a three-dimensional facial scanning system based on structured light techniques.* Comput Methods Programs Biomed, 2009. 94(3): p. 290-8.

27. van Lindert, E.J., et al., *Validation of cephalic index measurements in scaphocephaly.* Childs Nerv Syst, 2013. 29(6): p. 1007-14.

28. Morita, Y., et al., *Technical note: Quantification of neurocranial shape variation using the shortest paths connecting pairs of anatomical landmarks.* Am J Phys Anthropol, 2013. 151(4): p. 658-66.

29. Taylor, J.A. and T.A. Maugans, *Comparison of spring-mediated cranioplasty to minimally invasive strip craniectomy and barrel staving for early treatment of sagittal craniosynostosis.* J Craniofac Surg, 2011. 22(4): p. 1225-9.

30. Windh, P., et al., *Spring-assisted cranioplasty vs pi-plasty for sagittal synostosis--a long term follow-up study.* J Craniofac Surg, 2008. 19(1): p. 59-64.

31. Seruya, M., et al., *Computed tomography-based morphometric analysis of extended strip craniectomy for sagittal synostosis.* J Craniofac Surg, 2014. 25(1): p. 42-7.

8. Figure captions

Figure 1. Schematic representation of the positioning of the craniotomy (square), osteotomies (dashed line) and springs positioned in small notches in the parietal bone.

Figure 2. a) Example of the raw 3D surfaces of a patient acquired with the handheld scanner at follow-up; b) clean surface of the same patient after deleting unwanted structures and removal of irregularities due to the stocking; c) cutting plane position through nasion and both left and right tragion, and d) final STL file after cutting and closure of the mesh around the ears. For morphometric analysis, the head circumference is represented by the black solid line, the sagittal length over the head by the dashed line and the coronal width from left to right tragion by the double dotted dashed line.

Figure 3. Examples of artefacts and voids in suboptimal surface acquisitions.

Figure 4. Bland-Altman plot of agreement between CI measured on x-ray and 3D scan.

Figure 5. Population mean cephalic index measured on 3D scans with error bars of one standard deviation (SD). CI increased significantly (Table 2) from pre-op to post-op, from pre-op to follow-up and from post-op to follow-up.

Figure 6. Population means of circumference, sagittal length, coronal width and volume at the three time-points with error bars of 1SD. Significant differences are reported in Table 2.

Figure 7. Bird's-eye view showing (facing to the right) the scans of the 9 patients pre-operatively (left column) and with colour maps of the changes from the pre-operative shape at the immediate post-op (central column) and at 3-week follow-up (right column).

Figure 8. 3D mean head shape from the population using SSM at the three time points. The changes from the pre-operative mean model are plotted in the colour maps for the post-op and follow-up mean models in bird's-eye view.

Figures

Figure 1

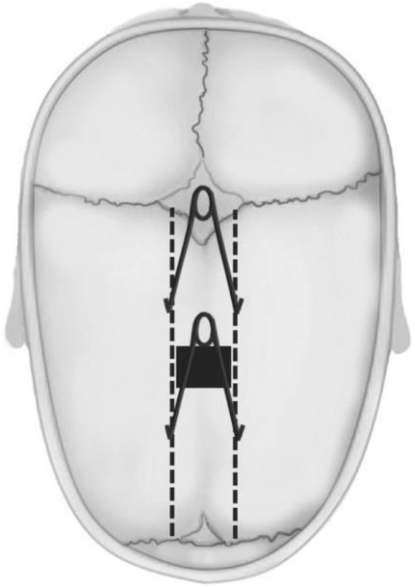

Figure 2

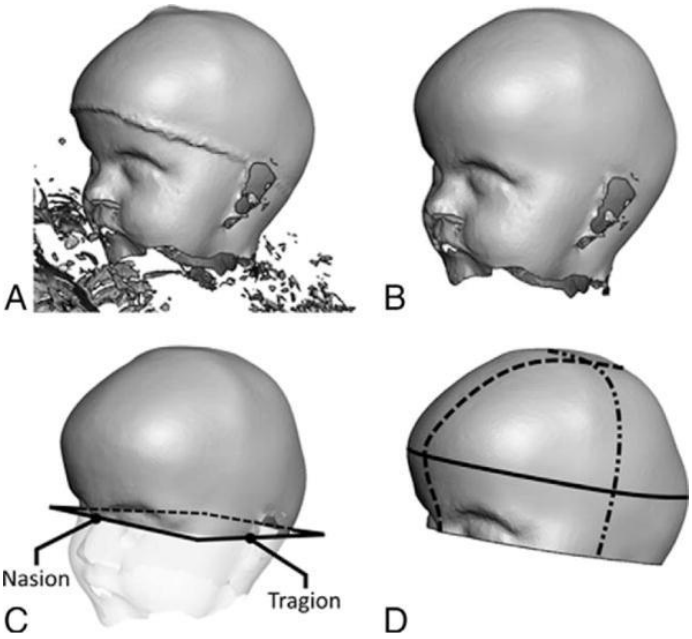

Figure 3

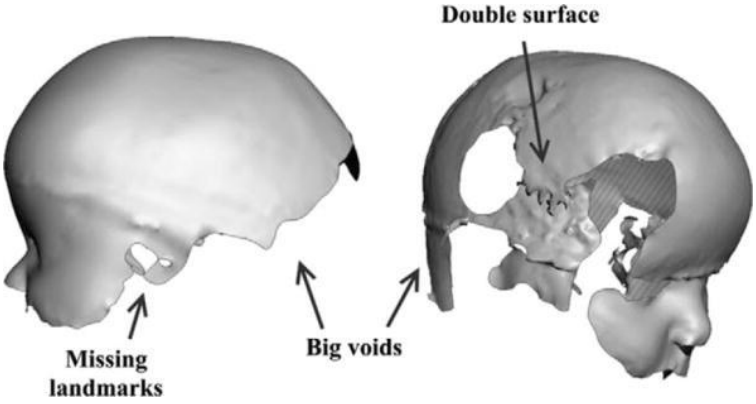

Figure 4

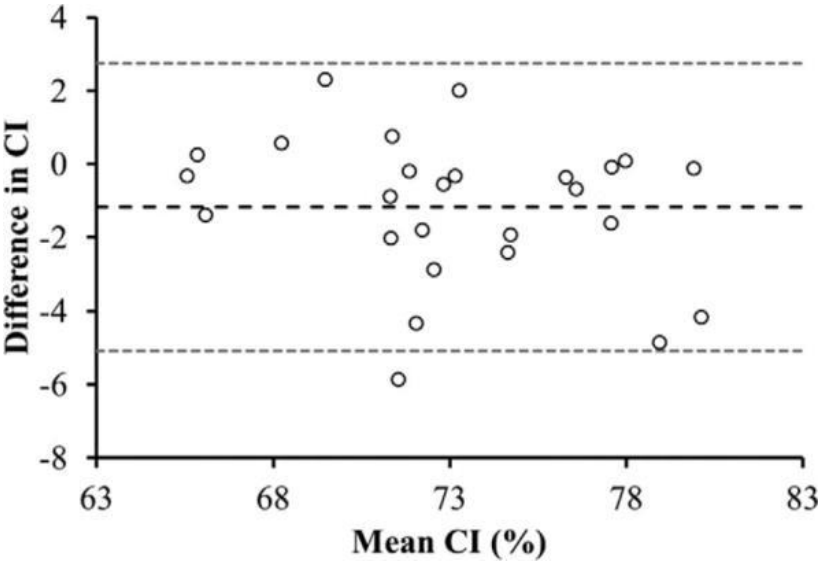

Figure 5

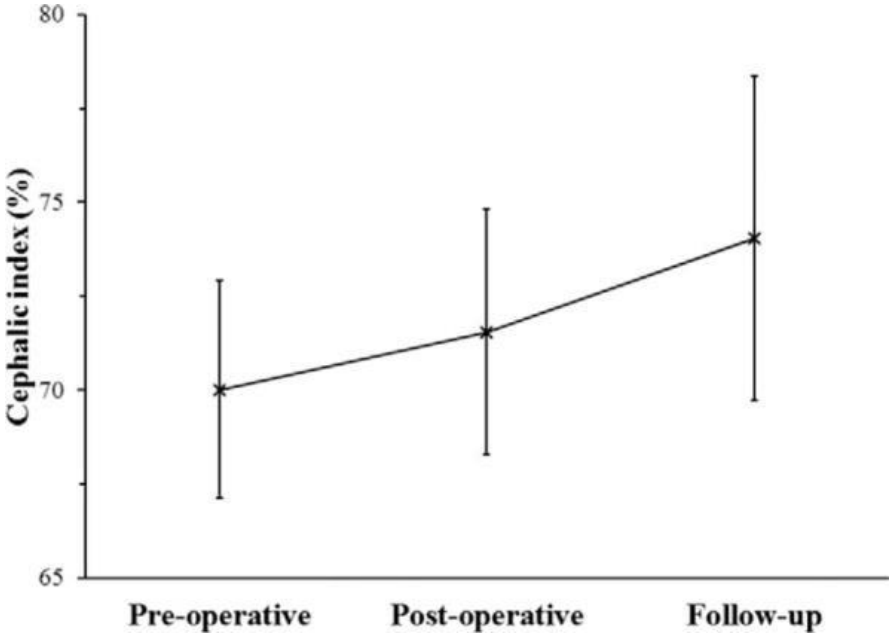

Figure 6

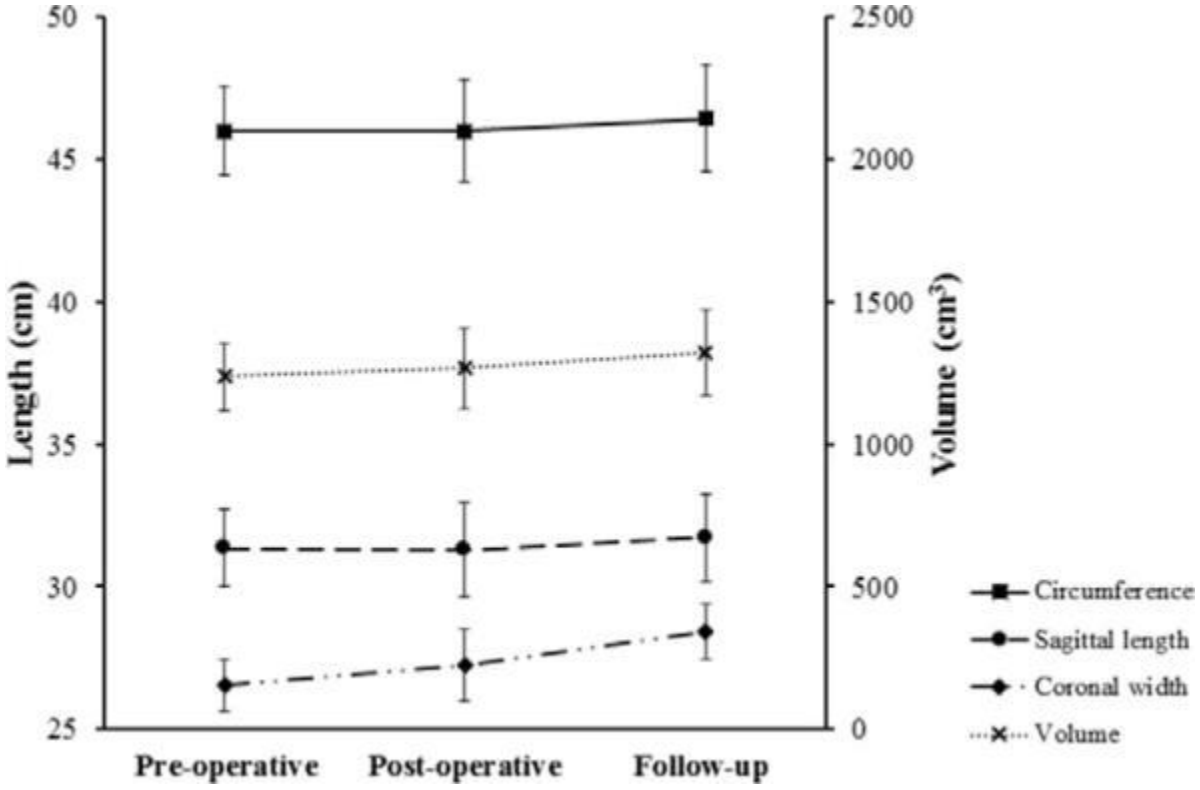

Figure 7

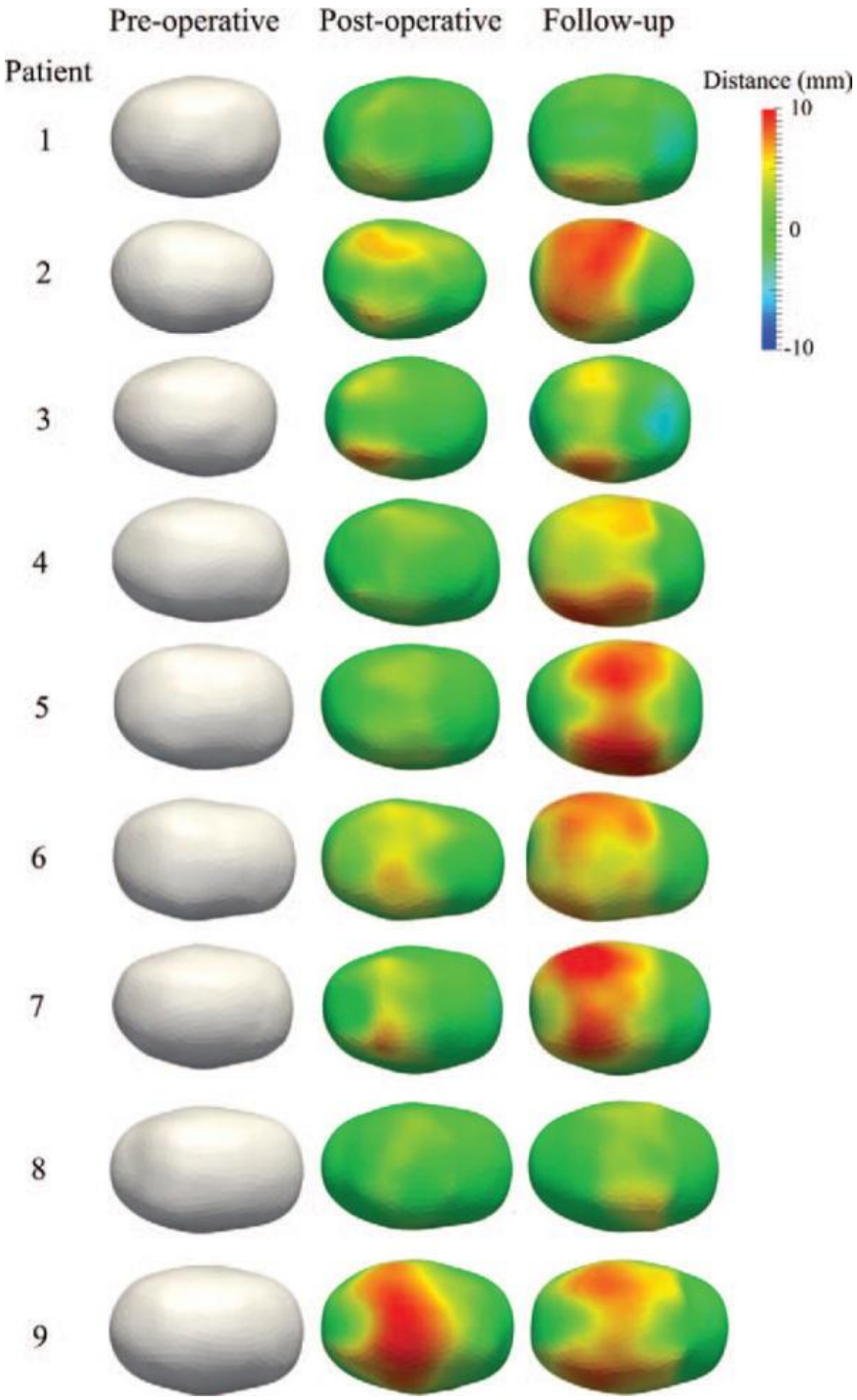
Pre-operative
Post-operative
Follow-up
Patient
1
2
3
4
5
6
7
8
9
Distance (mm)
10
0
-10

Figure 8

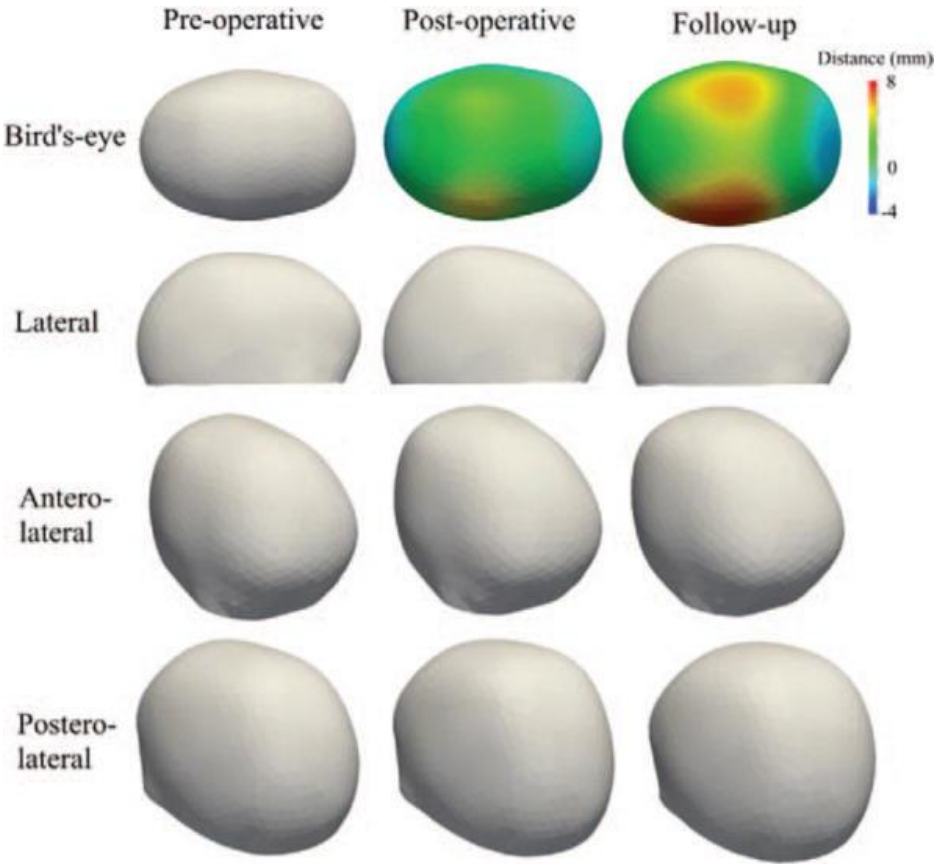
Pre-operative
Post-operative
Follow-up
Distance (mm)
8
0
-4
Bird's-eye
Lateral
Antero-lateral
Postero-lateral

Tables

Table 1: Patient population demographics and spring cranioplasty information.

				Anterior Spring			Posterior Spring		
					Opening (mm)			Opening (mm)	
Patient	Sex	Age at Surgery (Mo)	Surgery to FU (Days)	Model	Post-op	FU	Model	Post-op	FU
1	M	4.0	17	S12	33	54	S12	43	55
2	M	4.1	31	S12	38	57	S12	42	58
3	M	4.4	22	S12	39	55	S12	43	55
4	M	4.9	27	S12	39	56	S12	43	57
5	M	5.0	22	S14	29	49	S14	32	54
6	M	5.6	17	S12	31	55	S14	33	54
7	M	5.7	22	S12	38	59	S12	38	51
8	F	6.1	20	S14	35	55	S14	34	45
9	M	7.2	17	S14	38	55	S14	42	55

S12 and S14 indicated the spring models implanted in each patient in the anterior and posterior position; opening of the springs was measured on the operating table just after insertion and from x-rays at 3 week follow-up.

F, female; FU, follow-up; M, male.

Table 2: P-values of differences in CI, Volume, Coronal, and Sagittal Length, and Circumference from Pre-Op to Post-Op, from Pre-Op to Follow-Up, and from Post-Op to Follow-Up.

	P Value		
	Pre–Post	Pre–Follow-Up	Post–Follow-Up
Cephalic index	0.011*	0.008*	0.011*
Volume	0.028*	0.008*	0.011*
Coronal width	0.012*	0.012*	0.015*
Sagittal length	0.889	0.401	0.260
Circumference	1.000	0.093	0.028*

*$P < 0.05$.